




Article

# Active Power Management of Virtual Power Plant under Penetration of Central Receiver Solar Thermal-Wind Using Butterfly Optimization Technique

Partha Pratim Dey <sup>1</sup>, Dulal Chandra Das <sup>1</sup>, Abdul Latif <sup>1,\*</sup>, S. M. Suhail Hussain <sup>2</sup> and Taha Selim Ustun <sup>2</sup>

<sup>1</sup> Department of Electrical Engineering, National Institute of Technology Silchar, Assam 788010, India; parthapratim.rst@gmail.com (P.P.D.); dulal@ee.nits.ac.in (D.C.D.)

<sup>2</sup> Fukushima Renewable Energy Institute, AIST (FERA), National Institute of Advanced Industrial Science and Technology (AIST), Koriyama 963-0298, Japan; suhail.hussain@aist.go.jp (S.M.S.H.); selim.ustun@aist.go.jp (T.S.U.)

\* Correspondence: abdul\_rs@ee.nits.ac.in

Received: 15 July 2020; Accepted: 25 August 2020; Published: 27 August 2020



**Abstract:** Striving for the suppression of greenhouse emissions, the modern power network is facing fundamental changes with the utilization of renewable energies (REs) for the future carbon-free society. The utilization of intermittent renewable-green power needs a better power management system and virtual power plant (VPP) can be a vital candidate that meets this demand. This study investigates a coordinated control grid integrated virtual power plant (VPP) in the presence of Central Receiver Solar Thermal System (CRSTS), Wind Turbine Generator (WTG), and Electric Vehicle (EV). To this end, CRSTS employed with thermal storage acts as a dispatchable renewable generating unit and coordinated control of the system units are achieved using the available control strategy on interconnected microgrids in the modified form, employing communication time delay. The proposed control strategy employs the proportional-integral (PI) and PI-derivative (PID) controller. Coordinated power control with real-time communication delay in grid integrated VPP in presence of CRSTS, WTG, and EV is a novel approach. Genetic algorithm (GA), Particle Swarm Optimization (PSO), Slap Swarm Algorithm (SSA), and recent Butterfly Optimization Algorithm (BOA) are used for tuning the necessary control parameters. The results establish the superiority of the BOA over SSA and PSO in suppressing system frequency deviations and tie line power deviation. The analysis of the dynamic response reveals that the consideration of the communication delay in the system expressively impedes the stable operation of the power system.

**Keywords:** central receiver solar thermal system (CRSTS); virtual power plant (VPP); frequency regulation; communication time delay; threshold time delay; butterfly optimization algorithm (BOA)

## 1. Introduction

Recent developments in power systems have led to more complex dynamic networks and have radically revolutionized the very concept of the conventional power system. In particular, the increased deployment of renewable energy (RE) sources and higher propagation of prosumers [1] into electricity networks are encouraged for curbing global warming and reducing fossil fuel use. However, due to certain socio-technical drawbacks and intermittent nature of RE sources, their integration creates issues in power system operation. Maintaining power quality, ensuring reliability and stability become a challenging task. As a solution, several RE units aggregated as a single entity have emerged as a

conventional generating unit that can make the job easier. Such aggregation is called virtual power plant (VPP). Although there is no comprehensive definition and definite structure of a VPP, there are some general conceptual designs. It is a cluster of distributed energy resources (DERs), storage units, controllable or flexible loads that together operate as a conventional generator [2]. The electric vehicle (EV) is one of the storage devices which can act as a controllable load also.

Meanwhile, it has been projected that the worldwide energy demand would increase to 1.5 times the present value by 2030 [3]. Further, most of the countries are bound to cut CO<sub>2</sub> emissions so as to arrest the global average temperature increase below 2 °C, as per the Paris agreement [4]. In order to meet the above two challenges, a major portion of the world energy requirements should be supplied by RE sources. Amongst the available RE sources, like wind energy systems, the central receiver solar thermal system (CRSTS) is also promising technology that has the potential to provide significant dispatchable power. Especially during a cloudy day or night time, the thermal storage capability makes the system available for generation [5]. The presence of thermal storage absorbs the intermittent nature of output power generation. Further, because of its capability to operate at high temperature and lesser land requirements as compared to other technologies, CRSTS has gained much popularity. These benefits of CRSTS make it a carbon-free and sustainable energy solution. The state of the art of CRSTS technology has been discussed in [6]. Although the cost of this concentrated solar thermal power at present is costlier than that of other renewable technology, with significant technological development and large-scale generation, the generation cost of this technology is expected to be on par with the thermal generation [5]. To this end, several countries are working towards development of this technology that would make CRSTS a vital candidate for VPP application.

VPP is supported by information and communication technology (ICT) [7], and improves stability, reliability, and resiliency by tailoring the plethora of RE sources spreading over the geographical areas, while providing other benefits [8,9]. For instance, through proper coordination of the RE sources, storage capacity, and controllable loads, VPP may ensure stable operation and peak load reduction. Additionally, VPP allows market participation for prosumers, and provides auxiliary services [10]. In ancillary service, voltage and load-frequency control are two important strategies that are essential in maintaining power system stability [11]. Although VPPs are likely to play a vital task in future energy systems through the aggregation of DERs and storage devices, developing control strategies for proper operation is a challenging task [12]. This is because of the integration of RE sources which are stochastic in nature due change in the weather conditions. The output power variations of RE sources give rise to imbalance between the power generation (active and reactive) and load demand, which result in frequency and voltage fluctuations.

A conventional power system with high inertia is of bulk capacity; integration of RE sources or EV in such a power system may not create much fluctuation in frequency. While a microgrid with low capacity has less system inertia, when such a microgrid is integrated with RE sources or EV, the output power fluctuation may crease the system frequency fluctuation. However, integrating the microgrid with the VPP architecture may resolve this issue to some extent. Nevertheless, the control concept strategy of VPP demands much attention.

Recent works on VPP [13–19] emphasize the requirement of frequency regulation in power system networks with high penetration of renewable sources or DERs. A VPP with a robust and efficient energy management system (EMS) has the potential to address this need [13]. VPP allows dynamic participation of DER, prosumers, and energy storage system (ESS) to maintain the demand-supply balance of the grid at different time scales [14,15]. Necessary market participation steps were studied in [16,17]. Hierarchical control strategies and coordinated EMS algorithm for generation command dispatch amongst the VPP participants towards system frequency stabilization were studied in [18]. VPP was reported to use some optimization tools and controller design for containment of frequency fluctuation in the electrical power system [19]. Authors in [20] focused on direct load control approach for consumers to participate in VPP-based electricity markets. In [21], authors presented Hybrid Automata (HA) for modeling of VPP with a conceptual control strategy in the presence of combined

heat and power (CHP), battery, wind, and solar photovoltaic (PV). Although certain literature has reported RE-based VPP control strategies, there is still ongoing research to develop a mature control structure similar to those in conventional power system. It has been stated that VPPs are usually operated in grid-connected mode, as the isolated operation may not be feasible. Controlling DERs in VPP is akin to the secondary control approach of microgrids that takes comparatively higher time for control action as compared to primary control strategy [18]. Therefore, VPP can make use of ICT that causes certain time delay. These communication delays play a significant role in VPP design, operation, and analysis, as longer delays could be detrimental to the power system's health [22]. Therefore, in the context of VPPs, communication delay needs to be set appropriately by finding the time-lag required before regulatory action is introduced to contain the power imbalance and oscillations.

Meanwhile, optimization techniques and control strategies for microgrid/interconnected have also attracted research attention. Several optimization techniques, such as genetic algorithmic technique (GA) [18,23], Particle Swarm Algorithmic technique (PSO) [24], and social spider algorithmic technique (SSA) [25] have been researched to this end. Recently, butterfly optimization algorithm (BOA) was reported to provide a better solution in solving several complex engineering problems compared to other metaheuristic algorithms [26]. Therefore, the performance of the BOA may be explored in providing better tuning of controllers' parameters and hence better frequency regulation of the VPP model.

Recent research on control strategies for interconnected microgrids has been reported in [27–29]. In [27], the authors considered the *fmincon* solver method, a Matlab function and compared the performance with the proportional–integral–derivative (PID) based control strategy. The grasshopper optimization technique-fuzzy PID-based control strategy [28] and comparative performance of social-spider tuned PID control strategy vis-a-vis GA tuned PID control strategy were investigated in [29]. GA, PSO, sine-cosine algorithm, and Grasshopper optimization algorithm tuned PID control strategy were researched in [30]. The communication delay is significant for the realization of such interconnected microgrid system operation, because when this delay exceeds a threshold value, the microgrid may oscillate and may lose stability [31]. Therefore, for better realization of interconnected microgrids, communication delay (time required for receiving and sending information between the control center and the devices) should have been incorporated.

In light of the above, the present work develops a control strategy for VPPs based on control strategy of an interconnected microgrid [31]. The major contributions of this research work are:

- (a) The development of grid-integrated VPP in the presence of CRSTS, WTG, and EV and implementing it in MATLAB Simulation platform;
- (b) The application of available control strategy on interconnected microgrid in modified form for active power regulation of VPP model;
- (c) Considering communication delay in control system design and evaluations;
- (d) Use of a recent meta-heuristic optimization tool, namely BOA, for optimizing the control parameters and comparing the performance with GA, PSO, and SSA.

## 2. DER Modeling in VPP

The schematic structure of CRSTS is displayed in Figure 1. VPP design is illustrated in Figure 2, where DERs such as CRSTS, EV, and WTG are considered as Area-1 and a large conventional non-reheat turbine is considered as Area-2. The system components with respective mathematical models are illustrated below. The nomenclatures with values of some design parameters considered in this work are listed in Table 1.

### 2.1. Central Receiver Solar Thermal System (CRSTS)

CRSTS is one of the most appropriate DER types for VPP due to its potential and thermal storage capability. In particular, thermal energy storage capability responds to power demand fluctuations

while leveling the output variation due to stochastic nature of solar energy. CRSTS’s thermal electricity conversion efficiency is about 28% [32]. Worldwide, there are around 35 CRSTS projects in operation [3], with capacities in the order of MWs. Figure 1 shows the schematic diagram of a CRSTS.

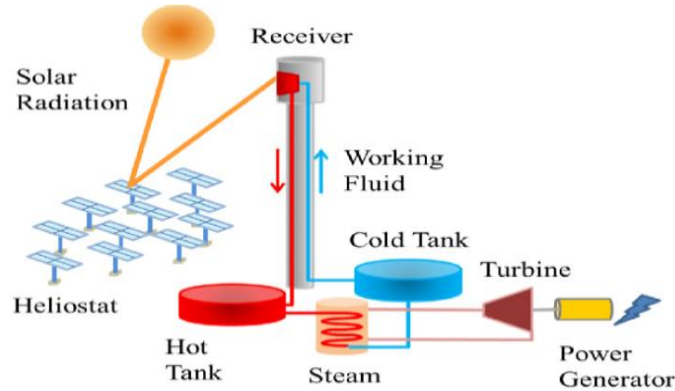


Figure 1. Schematic of a central receiver solar thermal system (CRSTS) [33].

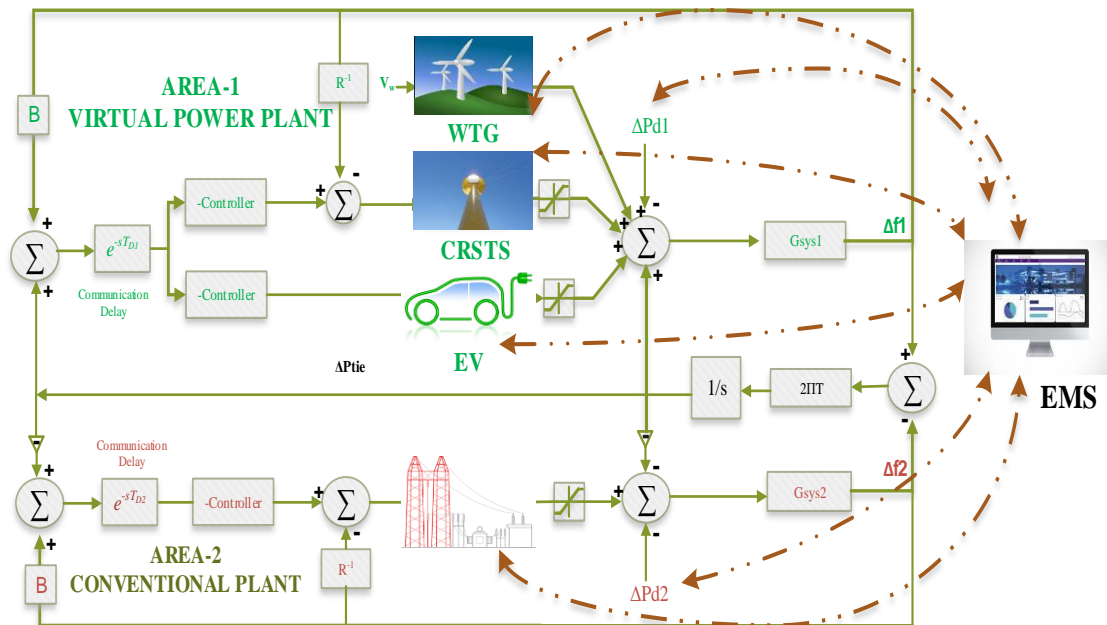


Figure 2. Schematic for Grid-Integrated VPP considering Communication Delay.

CRSTS converts sunshine to electricity. It operates by concentrating the solar rays to a central receiver using heliostats. A heat transfer fluid is heated and stored in storage tanks. As per the demand, the stored thermal energy is used to produce steam, which drives the turbine generator to produce clean energy. In the proposed work, the CRSTS is considered as a dispatchable power generator. The transfer function model of CRSTS is [34]:

$$G_{CRSTS}(S) = \left( \frac{K_{RF}}{1 + sT_{RF}} \right) \left( \frac{K_{RV}}{1 + sT_{RV}} \right) \left( \frac{K_G}{1 + sT_G} \right) \left( \frac{K_T}{1 + sT_T} \right), \tag{1}$$

where  $K_{RF}$ ,  $K_{RV}$ ,  $K_G$ ,  $K_T$  represent the gain of the refocus, receiver, governor, and turbine of CRSTS, respectively. The  $T_{RF}$ ,  $T_{RV}$ ,  $T_G$ ,  $T_T$  are the time constants of refocus, receiver, governor, and turbine of CRSTS.

**Table 1.** Nomenclature with considered systems' symbols values [34].

Nomenclature		Value
$K_{RF}, K_{RV}, K_G, K_T$	Gains of refocus, receiver, governor and turbine of CRSTS	1, 1, 1, 1
$T_{RF}, T_{RV}, T_G, T_T$	Time of refocus, receiver, governor, and turbine of CRSTS	1.33 s, 4 s, 0.08 s, 1 s
$K_{WTG}, T_{WTG}$	Gain and time constant of WTG	1, 1.5 s
$K_{Td}, T_{Td}$	EV gain and time constant	1, 0.15 s
$T_{G1}, T_{T1}$	Gain and delay of conventional generator	0.08, 0.3 s
$R_1, R_2$	Constant droop value of area-1, 2	2.4 Hz/p.u MW
$B_1, B_2$	Biasing constant of area-1, 2	0.429, 0.424
$K_{sys1}, K_{sys2}$	System characteristics	1120
$M_1 \& M_2$	Moment of inertia of the VPP and Conventional Generator.	0.2 s, 0.166 s
$D_1 \& D_2$	Damping constant of the VPP and Conventional Generator.	0.012, 0.008 (p.u MW/Hz)
$T_{D1}, T_{D2}$	Communication delay for VPP and Conventional plant	1.2 s, 1 s
$T_{12}$	Synchronizing tie-line co-efficient between area-1 and 2	4.397

## 2.2. Wind Turbine Generator (WTG)

The wind turbine unit is one of the fastest growing renewable energy technologies. Nowadays, wind power has become the most important part of modern energy supply because of its capacity and availability. Energy conversion from wind to electricity is done by a wind turbine system, which includes a rotor with blades, gearbox, electrical generator, and power electronics component. The power output of the wind turbine depends on the speed of wind at that instant. Wind turbines contain several nonlinearities, so while modeling this must be considered. The wind turbine model is simplified into a first order system. The transfer function of WTG based on modeling in [23] is expressed by following equation:

$$G_{WTG}(s) = \frac{K_{WTG}}{T_{WTG}s + 1} \quad (2)$$

where  $K_{WTG}$ ,  $T_{WTG}$  are the gain and time constant of WTG.

## 2.3. Electric Vehicle (EV)

The electric vehicle is the most promising technology that provides a solution to the environmental issues by reducing CO<sub>2</sub> emissions [35,36], and at the same time minimizes the use of oil on a per kilometer basis. EVs can work as an energy storing device to absorb renewable energy and provide support to grid service when it is plugged-in. The bidirectional connection capability of converters in EVs' structure has made them a secure backup for frequency support in power systems. The model which is used in this paper is the first order system. The transfer function model of EV based on modeling in [37] is expressed by the following equation:

$$G_{EV}(s) = \frac{1}{T_{Td}s + 1} \quad (3)$$

where  $T_{Td}$  is the time constant of EV.

## 2.4. Conventional Synchronous Generator

The non-reheat turbine is one of the proficient and flexible machines which are capable of fulfilling a wide range of steam cycle applications. In this paper, the conventional plant used is not a reheat turbine type and the non-reheat turbine consists of three parts and their transfer function models are: Governor with Dynamics:

$$G_g(s) = \frac{1}{T_{G1}s + 1}; \quad (4)$$

Turbines with Dynamics:

$$G_t(s) = \frac{1}{T_{T1}s + 1}; \quad (5)$$

Load and Machine Dynamics:

$$G_p(s) = \frac{K_p}{T_{ps} + 1}; \quad (6)$$

where  $T_{RF}$ ,  $T_{RV}$  represent the time constant of conventional generator and turbine, and the overall conventional system's gain and time constant are depicted by  $K_p$  and  $T_p$ .

### 2.5. Information and Communication Technology (ICT)

Future VPPs would connect millions of prosumers, DERs including REs, energy-storing devices, and a plethora of energy-consuming appliances. It would essentially allow two-way communication for receiving and sending information regarding running status, energy management, analysis, conveying control signals to all the VPP system components. This could only be achieved by profound application of information and communication technologies (ICT). Hence, it is highly likely that ICT would become one of the most essential VPP research topics. ICT such as internet of things or cloud-based infrastructure are the emerging technologies. The ICT network takes certain time for communicating information, e.g., for receiving/sending data from/to the control center and the VPP system components, called communication delay. In this work, the communication delay required for receiving as well as sending information is approximated to a single delay and implemented in the controller forward loop.

The transfer function model of communication delay  $e^{-sT_D}$  using Pade 1st order approximation [22,38] is represented in the following form:

$$e^{-sT_D} = \frac{-\frac{1}{2}sT_D + 1}{\frac{1}{2}sT_D + 1}, \quad (7)$$

where  $T_D$  is the delay time.

## 3. Methodology

### 3.1. Formation of the Objective Function

The main objective of the VPP is to maintain a demand-supply balance, irrespective of random variations in RE generation and load. To this end, in association with ICT and appropriate control strategy, VPP minimizes the power imbalance. Therefore, an integral of the squared error (ISE) of the frequency deviation of VPP, tie-line, and main grid frequency deviation is taken as the objective function ( $J$ ), which is expressed as follows:

$$\text{Minimize } J_{ISE} = \int_0^{t_{sim}} [(\Delta f_1)^2 + (\Delta f_2)^2 + (\Delta P_{tie})^2] . dt. \quad (8)$$

It is subject to:

$$\begin{cases} K_p^{\min} \leq K_p \leq K_p^{\max} \\ K_I^{\min} \leq K_I \leq K_I^{\max} \\ K_D^{\min} \leq K_D \leq K_D^{\max} \end{cases}, \quad (9)$$

where,  $K_p$ ,  $K_I$ , and  $K_D$  in are the parameters of the PID controller. By using popular optimization techniques GA, PSO, SSA, and recently BOA, the gains of PI and PID controllers are optimized to study the proposed system responses.

### 3.2. Adopted Control Strategy

The VPP must provide control signal to the DERs so as to keep supply-demand balance. To this end, researchers have favored a centralized control concept amongst the available architectures, such as



distributed and hybrid control [18]. In centralized control, the VPP possesses the status of the DERs; accordingly, the central controller dispenses signal corresponding to target power demand from the DERs. The EMS in VPP manages the prosumers' resources such as controllable load, for instance, EV charging stations and DERs. The vehicle to grid mode of EV, WTG, and CTSTS is the DERs to be monitored by the EMS. Controllers employed with the CTSTS and EV do the necessary supervisory control action to virtualize the VPP. EMS interacts and sends signals to the controllers so as to adjust the power generation and maintain a power balance. PI and PID controllers have been employed for the control system. The controller input is the frequency deviation of the system. The GA, PSO, SSA, and BOA are used to design the controller for the model. The results of the algorithms have been compared and analyzed separately after simulation. BOA is discussed in the following section, while PSO and SSA are well documented in the literature [24,25].

### 3.3. Overview of Butterfly Optimization Algorithm (BOA)

In the VPP model, generating units are employed with the controllers (PI/PID). The parameters of these controllers are optimized using GA, PSO, SSA, and the recently developed BOA. GA, PSO, and SSA are detailed in references [23–25], respectively, so the authors present only BOA in the present paper.

Recently, in 2018, Arora and Singh developed a Butterfly Optimization algorithm (BOA) by utilizing the food searching strategy and mating behavior of butterflies [26]. The optimization function considers butterflies as search agents [39]. The entire conception of sensing and processing the modality depends on three important factors viz. sensory modality 'c', stimulus intensity 'I', and power exponent 'a'. The sensory modality is fragrance, 'I' is the magnitude of the physical stimulus and the parameter 'a' allows for regular expression, linear response, and response compression in BOA. Using these concepts, in BOA, the fragrance is formulated as a function of the physical intensity of stimulus as follows:

$$f = cI^a, \quad (10)$$

where 'f' is the perceived magnitude of the fragrance, i.e., how much stronger the fragrance is perceived by other butterflies. We can consider 'a' and 'c' in the range [0, 1] for our study. The algorithm has two key steps, viz., global search phase and local search phase. In global search phase, the butterfly takes a step toward the fittest butterfly/solution 'g\*', which is represented by the following equation:

$$x_i^{t+1} = x_i^t + (r^2 \times x_j^t - x_k^t) \times f_i, \quad (11)$$

where  $x_i^t$  is the solution vector  $x_j$  for  $i$ th butterfly in iteration number 't'. Here,  $g^*$  represents the current best solution found among all the solutions in current iteration. Fragrance of  $i$ th butterfly is represented by  $f_i$  and  $r$  is a random number in [0, 1].

Local search phase can be represented as:

$$x_i^{t+1} = x_i^t + (r^2 \times g^* - x_i^t) \times f_i, \quad (12)$$

where  $x_j^t$  and  $x_k^t$  are  $j$ th and  $k$ th butterflies from the solution space. If  $x_j^t$  and  $x_k^t$  belong to the same swarm and  $r$  is a random number in [0, 1], then Equation (12) becomes a local random walk. The corresponding flow diagram of BOA technique is displayed in Figure 3. The considered system parameters are tabulated in the Appendix A.

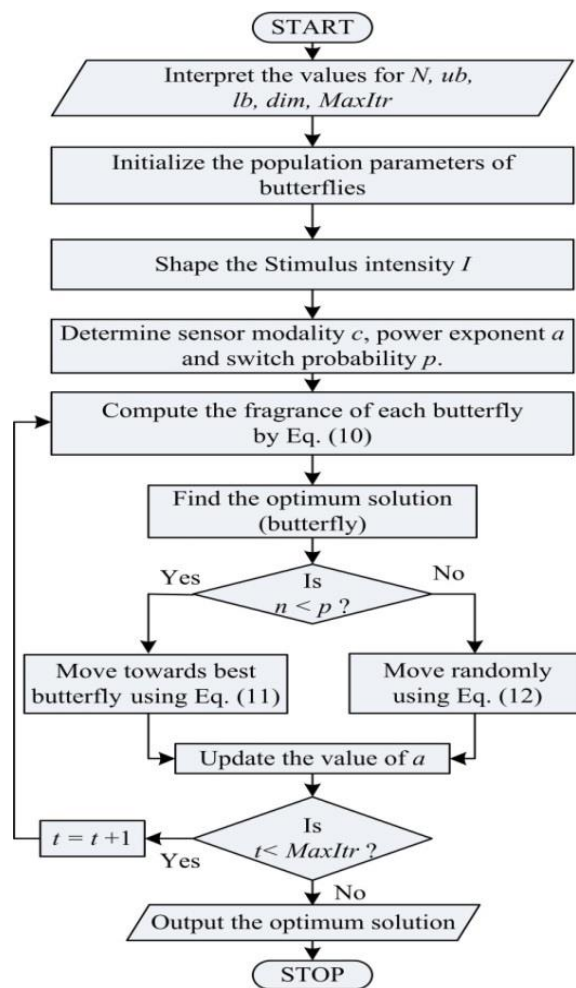


Figure 3. Flow diagram of the BOA technique.

#### 4. Simulated Results and Analysis

In order to investigate the system response, the proposed system shown in Figure 2 was modeled and simulated in MATLAB. System conditions detailed in Table 2 were enforced and three different optimization techniques were utilized to benchmark their performances.

Table 2. Operating conditions for an interconnected VPP system.

Case	Subsystem	Simulation Time (s)	Operating Condition
Case-1: for comparison between PI and PID controller performance			$P_{WTG} = 0.1$ p.u. at $0 < t < 20$ s $= 0.11$ p.u. at $t > 20$ s
Case-2: for comparison of optimization algorithms GA, PSO, SSA and BOA	CRSTS, WTG, DEG, PHEV and load	100	$P_{dl} = 0.02$ p.u. at $0 < t < 40$ s $= 0.03$ p.u. at $40 < t < 60$ s $= 0.05$ p.u. at $t > 60$ s
Case-3: for comparison of dynamic response with increased time delay attacks			Communication time delay for Area-1 is $T_{D1} = 1.2$ s and for Area-2 is $T_{D2} = 1$ s

##### 4.1. Time Domain Analysis of the VPP Model Employed with PI and PID

The time domain analysis obtained by simulation of the MATLAB Simulink model (Figure 2) is shown in Figures 4–6. Controller parameters in this case were optimized using particle swarm optimization algorithms (PSO). From the responses  $\Delta f_1$ ,  $\Delta f_2$ , and  $\Delta P_{tie}$ , as presented in Table 3,



it was observed that the PI controlled system has higher overshoot, under-shoot, and settling time as compared to the PID controlled system. Because of the derivative term in PID controller, it acts faster to the system disturbance in the VPP and the EMS system sets the appropriate coordination between the DERS to cater the demand, which in turn contains frequency fluctuation.

**Table 3.** Peak over-shoot, under-shoot, and settling time for PI and PID controller parameters optimized using PSO.

Case-1	Response	Peak over Shoot (H.z)	Peak Under-Shoot (H.z)	Settling Time (s)
PI	$\Delta f_1$	0.04019	0.01149	90.00
	$\Delta f_2$	0.03882	0.01101	89.36
	$\Delta P_{tie}$	0.01635	0.00459	89.58
PID	$\Delta f_1$	0.01796	0.006509	83.65
	$\Delta f_2$	0.0159	0.004616	82.74
	$\Delta P_{tie}$	0.00658	0.002019	81.04

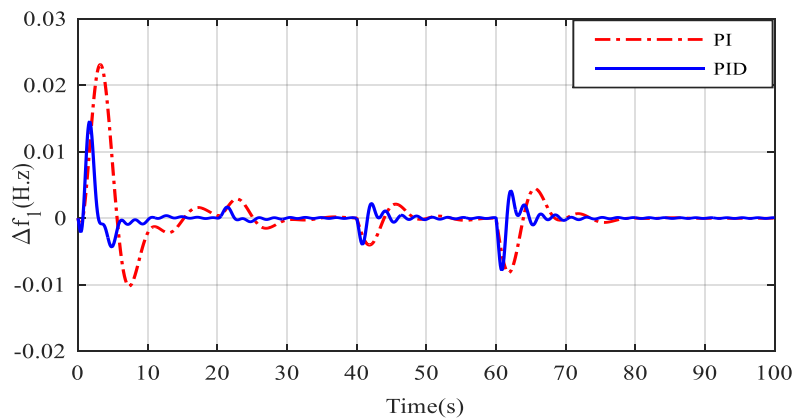


**Figure 4.**  $\Delta f_1$  for PI and PID.

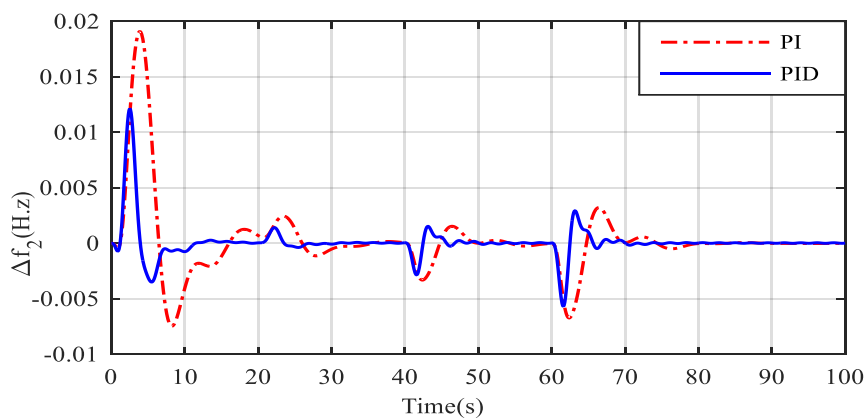


**Figure 5.**  $\Delta f_2$  for PI and PID.

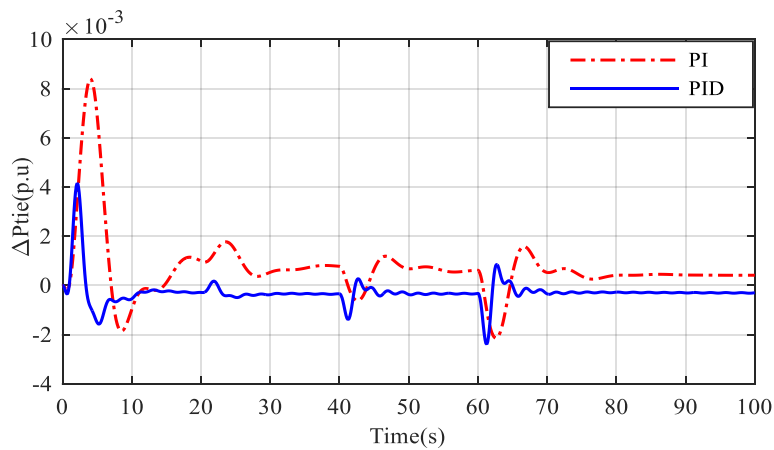


Figure 6.  $\Delta P_{tie}$  for PI and PID.

4.2. Time Domain Analysis for Optimization Algorithms GA, PSO, SSA, and BOA

The time domain analyses in Figures 7–9 were obtained by PID controller-based simulation of the proposed MATLAB Simulink VPP model using optimization algorithms PSO, SSA, and BOA. The responses of  $\Delta f_1$ ,  $\Delta f_2$ , and  $\Delta P_{tie}$  using GA, PSO, SSA, and BOA are illustrated, which show that the response in the case of BOA was better than GA, PSO, and SSA at all the times when changes occurred frequently in the system. It can be clearly seen from Table 4 that in the case of GA, PSO, and SSA, the overshoot, under-shoot, and settling time were more when the system was getting disturbed, but in the case of BOA, it showed better control over system controller parameters.

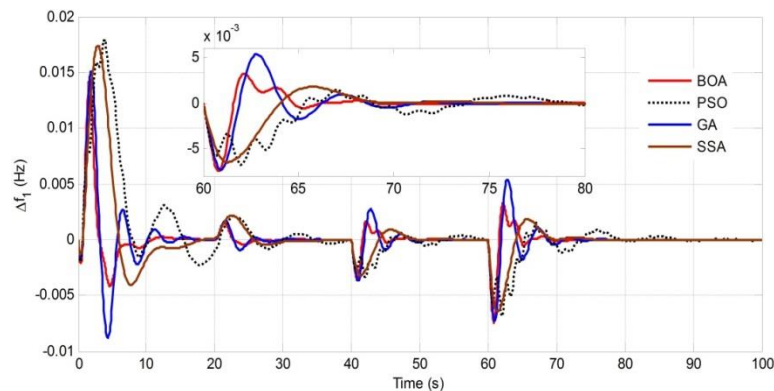


Figure 7.  $\Delta f_1$  under GA, PSO, SSA, and BOA.

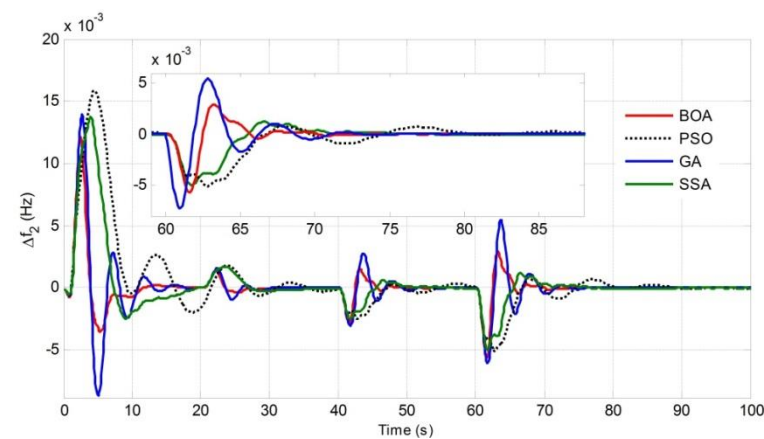


Figure 8.  $\Delta f_2$  under GA, PSO, SSA, and BOA.

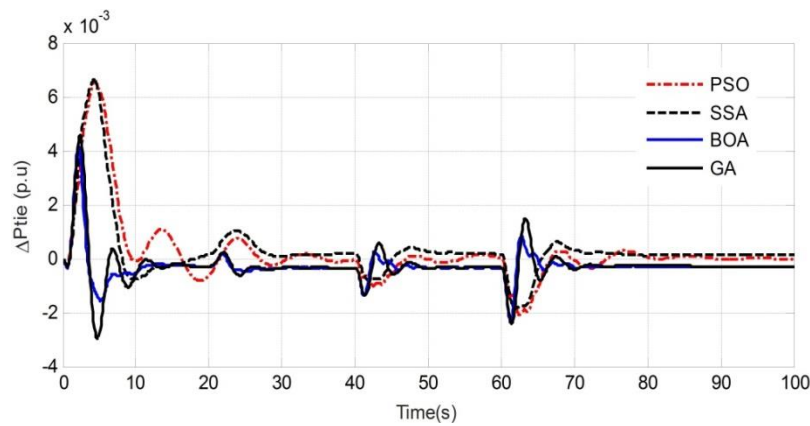


Figure 9.  $\Delta P_{tie}$  under GA, PSO SSA, and BOA.

This analysis interpreted that BOA-optimized PID controllers give a better result than the GA, PSO, and SSA optimized counterparts and illustrated the superiority of BOA over the GA, PSO, and SSA algorithms. Furthermore, the convergence curves of GA, PSO, SSA, and BOA as shown in Figure 10 also confirm the superiority of BOA over GA, PSO, and SSA.

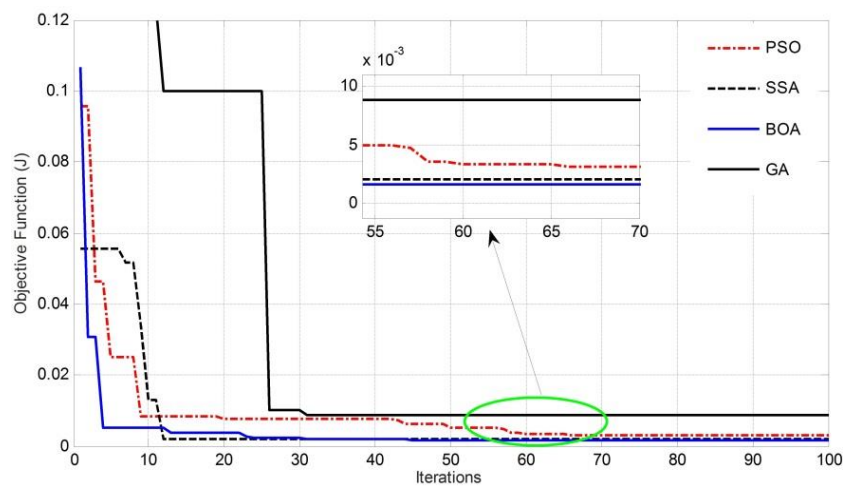


Figure 10. Comparative convergence curve under GA, PSO, SSA, and BOA.

Table 4. Peak over-shoot, under-shoot, and settling times for PID controller parameters optimized using GA, PSO, SSA, and BOA.

Case-3	Response	Peak over Shoot (H.z)	Peak Under-Shoot (H.z)	Settling Time (s)
GA	$\Delta f_1$	0.01498	0.00908	72.11
	$\Delta f_2$	0.01405	0.00912	74.24
	$\Delta P_{tie}$	0.00427	0.00309	73.85
PSO	$\Delta f_1$	0.01796	0.006509	83.65
	$\Delta f_2$	0.01590	0.004616	82.74
	$\Delta P_{tie}$	0.00658	0.002019	81.04
SSA	$\Delta f_1$	0.01730	0.006306	75.74
	$\Delta f_2$	0.01394	0.00528	75.54
	$\Delta P_{tie}$	0.00662	0.00176	75.25
BOA	$\Delta f_1$	0.01428	0.00757	70.30
	$\Delta f_2$	0.01217	0.00561	72.02
	$\Delta P_{tie}$	0.004153	0.00239	72.60

### 4.3. Time Domain Analysis of the VPP Model with Increasing Communication Delay ( $T_D$ )

The system stability is significantly influenced by communication delay,  $T_D$ . If the communication delay in a VPP exceeds a threshold value, it causes oscillations, and in the worst case may lead to instability. This section presents the comparative performance of the proposed MATLAB Simulink VPP model with increasing  $T_{D1}$ . Figures 11–13 represent  $\Delta f_1$ ,  $\Delta f_2$ , and  $\Delta P_{tie}$ , respectively, for a BOA-optimized PID controller for the proposed VPP model. The analysis of response for  $\Delta f_1$ ,  $\Delta f_2$ , and  $\Delta P_{tie}$ , in terms of the peak overshoot, peak under-shoot, and settling time reveal that as the time delay was increased from  $T_{D1} = 1.2$  s to  $T_{D1} = 1.4$  s stepwise (with a step of 0.1 s) system oscillation was also increased. However, the proposed control scheme regulates the system frequency deviations. The moment  $T_{D1}$  increases to 1.5 s, the system oscillation increased significantly as compared to that of the oscillation occurred at 1.2 s and the system seems to be on the verge of losing stability. Hence,  $T_{D1} = 1.4$  s could be considered as the threshold value of communication time delay and any value beyond this would impede the stable operation of the VPP. The Table 5 provides a quantitative representation of the increased system oscillations with the increase in the communication time delay in the system.

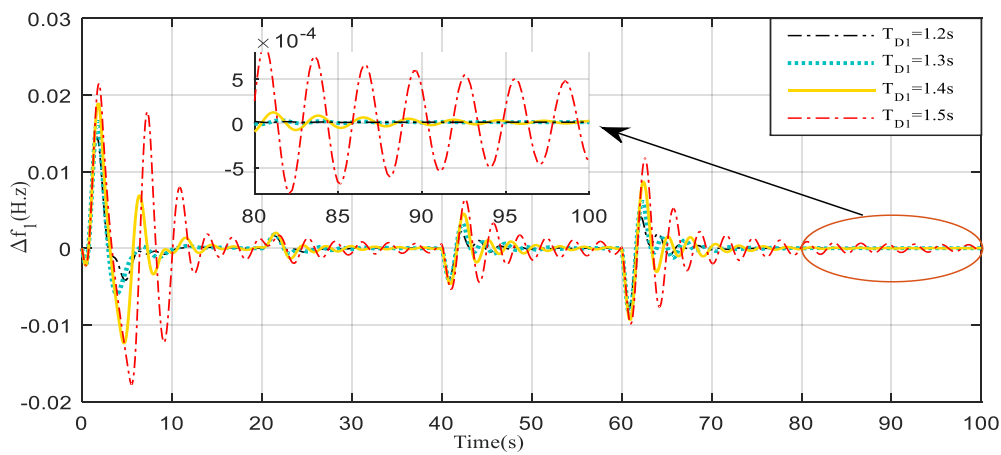


Figure 11.  $\Delta f_1$  with increasing communication delay.

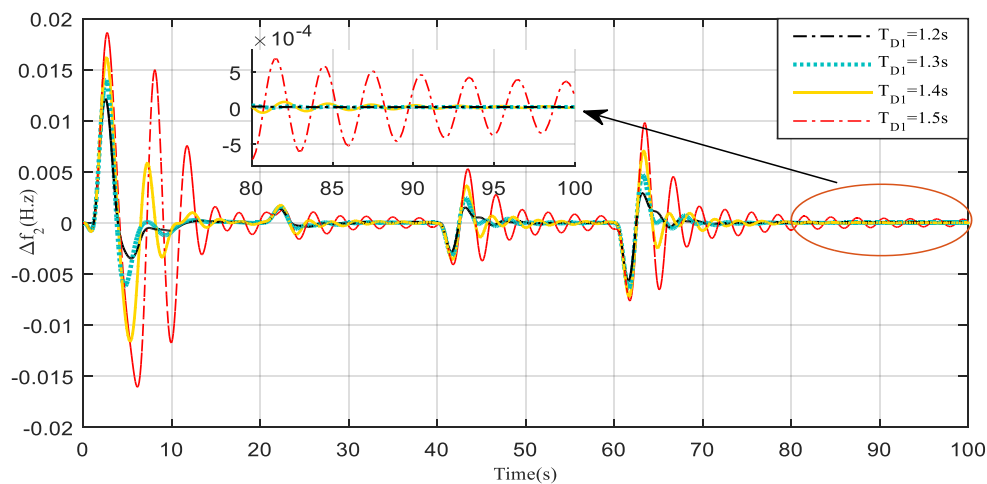


Figure 12.  $\Delta f_2$  with increasing communication delay.

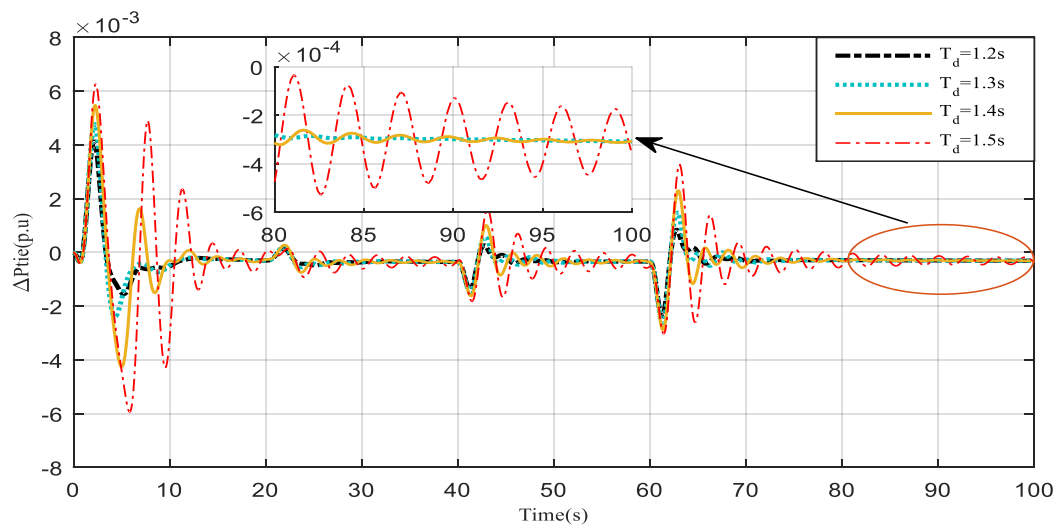


Figure 13.  $\Delta P_{tie}$  with increasing communication delay.

Table 5. Peak over-shoot, under-shoot, and settling time for BOA-optimized PID controller considering different time delays.

Time Delay Attacks	Response	Peak over Shoot (Hz)	Peak Under-Shoot (Hz)	Settling Time (s)
$T_{D1} = 1.2$ s	$\Delta f_1$	0.01428	0.00757	70.30
	$\Delta f_2$	0.01217	0.00561	72.02
	$\Delta P_{tie}$	0.004153	0.00239	72.60
$T_{D1} = 1.3$ s	$\Delta f_1$	0.01639	0.00857	74.6
	$\Delta f_2$	0.01397	0.00639	73.19
	$\Delta P_{tie}$	0.00477	0.00247	75.62
$T_{D1} = 1.4$ s	$\Delta f_1$	0.01894	0.0122	80.20
	$\Delta f_2$	0.01616	0.01137	80.10
	$\Delta P_{tie}$	0.00542	0.00408	80.26
$T_{D1} = 1.5$ s	$\Delta f_1$	0.02134	0.01738	Unsettled
	$\Delta f_2$	0.01864	0.01602	Unsettled
	$\Delta P_{tie}$	0.00622	0.00561	Unsettled

## 5. Conclusions

Dynamic control that is based on the VPP concept can enhance system dynamics of power systems. This may lead to an increase in the share of renewable energy, while improving the transmission efficiency and reliability at the same time. The present work investigated the capability of using VPP to regulate the grid frequency with high penetration of CRSTS, WTG, and EV. Furthermore, the effect of real-time communication delays in VPP operation were also considered and incorporated in the system design.

The proposed grid-integrated VPP model was developed in the MATLAB Simulation platform and the impact with communication delays on the performance of the frequency regulation of VPP was evaluated. Simulation results show that increased communication delay can significantly degrade the response and even make the system unstable in some cases. Communication time delay of 1.4 s was found to be acceptable and hence considered as the threshold value for the proposed model. Any value beyond this would impede the stable operation of the VPP. On the control strategy, the analysis of the results endorses the superiority of the PID over PI controller and also establishes the dominance of the new optimization tool, i.e., BOA, over GA, PSO, and SSA. Finally, it has been observed that the available control strategy on interconnected microgrid could be employed for active power regulation of grid-integrated VPP in modified form, incorporating the real-time communication delays. In our

future work we shall consider application of other controller, like fractional order PID controller in VPP control strategy.

**Author Contributions:** Conceptualization, P.P.D.; A.L., S.M.S.H., D.C.D. and T.S.U.; Methodology, P.P.D.; A.L., S.M.S.H., D.C.D. and T.S.U.; Software, P.P.D. and A.L.; Validation, P.P.D.; D.C.D. and A.L.; Formal Analysis, A.L., S.M.S.H., D.C.D. and T.S.U.; Writing—Original Draft Preparation, P.P.D.; A.L. and D.C.D.; Writing—Review and Editing, S.M.S.H., and T.S.U.; Visualization, P.P.D. and A.L.; Supervision, D.C.D.; Funding Acquisition, T.S.U. All authors have read and agreed to the published version of the manuscript.

**Funding:** This research received no external funding.

**Acknowledgments:** Authors would like to thank TEQIP-III NIT Silchar for providing technical support for this work.

**Conflicts of Interest:** The authors declare no conflict of interest.

## Abbreviations

REs	Renewable energies
VPP	Virtual power plant
CRSTS	Central receiver solar thermal system
WTG	Wind turbine generator
EV	Electric vehicle
GA	Genetic algorithm
PSO	Particle swarm optimization
SSA	Slap swarm algorithm
BOA	Butterfly optimization algorithm
DERs	Distributed energy resources
ICT	Information and communication technology
EMS	Energy management system
ESS	Energy storage system
PID	Proportional integral derivative
$T_D$	Communication time delay
ISE	Integral of the square error

## Appendix A

Butterfly technique: Number of search agents: 50, Total iterations: 100, Probability of switching = 0.8, Power component = 0.1, Sensor modality = 0.1.

Salp swarm technique: Number of search agents: 50, Total iterations: 100.

Particle swarm technique: Number of search agents: 50, Total iterations: 100, Weighting factors ( $W_{max}$ ,  $W_{min}$ ) = 0.9 and 0.1,  $C1 = 2$ ,  $C2 = 2$ .

Genetic algorithm: Number of nests: 50, Total iterations: 100, Probability of crossover = 0.8, Probability of mutation = 0.01.

## References

1. Strasser, T.; Andren, F.; Kathan, J.; Cecati, C.; Buccella, C.; Siano, P.; Leitão, P.; Zhabelova, G.; Vyatkin, V.; Vrba, P.; et al. A Review of Architectures and Concepts for Intelligence in Future Electric Energy Systems. *IEEE Trans. Ind. Electron.* **2014**, *62*, 2424–2438. [[CrossRef](#)]
2. Xin, H.; Gan, D.; Li, N.; Li, H.; Dai, C. Virtual power plant-based distributed control strategy for multiple distributed generators. *IET Control Theory Appl.* **2012**, *7*, 90–98. [[CrossRef](#)]
3. Praveen, R.P. Performance Analysis and Optimization of Central Receiver Solar Thermal Power Plants for Utility Scale Power Generation. *Sustainability* **2020**, *12*, 127.
4. Niñerola, A.; Ferrer-Rullan, R.; Vidal-Suñé, A. Climate Change Mitigation: Application of Management Production Philosophies for Energy Saving in Industrial Processes. *Sustainability* **2020**, *12*, 717. [[CrossRef](#)]
5. Du, E.; Zhang, N.; Hodge, B.M.; Wang, Q.; Kang, C.; Kroposki, B.; Xia, Q. The role of concentrating solar power toward high renewable energy penetrated power systems. *IEEE Trans. Power Syst.* **2018**, *33*, 6630–6641. [[CrossRef](#)]



6. Ho, C.K. Advances in central receivers for concentrating solar applications. *Sol. Energy* **2017**, *152*, 38–56. [[CrossRef](#)]
7. Nadeem, F.; Aftab, M.A.; Hussain, S.M.; Ali, I.; Tiwari, P.K.; Goswami, A.K.; Ustun, T.S. Virtual Power Plant Management in Smart Grids with XMPP Based IEC 61850 Communication. *Energies* **2019**, *12*, 2398. [[CrossRef](#)]
8. Yavuz, L.; Önen, A.; Muyeen, S.M.; Kamwa, I. Transformation of microgrid to virtual power plant—A comprehensive review. *IET Gener. Transm. Distrib.* **2019**, *13*, 1994–2005. [[CrossRef](#)]
9. Castillo, A.; Flicker, J.; Hansen, C.W.; Watson, J.P.; Johnson, J. Stochastic Optimization with Risk Aversion for Virtual Power Plant Operations: A Rolling Horizon Control. *IET Gener. Transm. Distrib.* **2018**, *13*, 2063–2067. [[CrossRef](#)]
10. Ramos, L.F.; Canha, L.N. Virtual Power Plants and Their Prospects. *Electr. Electron. Eng.* **2019**, 1–21. [[CrossRef](#)]
11. Zajc, M.; Kolenc, M.; Suljanović, N. Virtual power plant communication system architecture. In *Smart Power Distribution Systems Control, Communication, and Optimization*; Academic Press: London, UK, 2018; pp. 231–250.
12. Khorasany, M.; Azuatalam, D.; Glasgow, R.; Liebman, A.; Razzaghi, R. Transactive Energy Market for Energy Management in Microgrids: The Monash Microgrid Case Study. *Energies* **2020**, *13*, 2010. [[CrossRef](#)]
13. Obaid, Z.A.; Cipcigan, L.M.; Abraham, L.; Muhssin, M.T. Frequency control of future power systems: Reviewing and evaluating challenges and new control methods. *J. Mod. Power Syst. Clean Energy* **2018**, *7*, 9–25. [[CrossRef](#)]
14. Abbasi, E. Coordinated primary control reserve by flexible demand and wind power through ancillary service-centered virtual power plant. *Int. Trans. Electr. Energy Syst.* **2017**, *27*, e2452. [[CrossRef](#)]
15. Tavakkoli, M.; Adabi, J.; Zabihi, S.; Godina, R.; Pouresmaeil, E. Reserve Allocation of Photovoltaic Systems to Improve Frequency Stability in Hybrid Power Systems. *Energies* **2018**, *11*, 2583. [[CrossRef](#)]
16. Liu, Y.; Xin, H.; Wang, Z.; Gan, D. Control of virtual power plant in microgrids: A coordinated approach based on photovoltaic systems and controllable loads. *IET Gener. Transm. Distrib.* **2015**, *9*, 921–928. [[CrossRef](#)]
17. Pudjianto, D.; Ramsay, C.; Strbac, G. Virtual power plant and system integration of distributed energy resources. *IET Renew. Power Gener.* **2007**, *1*, 10–16. [[CrossRef](#)]
18. Vandoorn, T.L.; Zwaenepoel, B.; De Koning, J.D.; Meersman, B.; Vandeveldel, L. Smart microgrids and virtual power plants in a hierarchical control structure. In Proceedings of the 2011 2nd IEEE PES International Conference and Exhibition on Innovative Smart Grid Technologies, Manchester, UK, 5–7 December 2011; pp. 1–7.
19. Newman, G.; Mutale, J. Characterising Virtual Power Plants. *Int. J. Electr. Eng. Educ.* **2019**, *4*, 307–318. [[CrossRef](#)]
20. Ruiz, N.; Cobelo, I.; Oyarzabal, J. A direct load control model for virtual power plant management. *IEEE Trans. Power Syst.* **2009**, *24*, 959–966. [[CrossRef](#)]
21. Javaid, C.J.; Allahham, A.; Giaouris, D.; Blake, S.; Taylor, P. Modelling of a virtual power plant using hybrid automata. In Proceedings of the 9th International Conference on Power Electronics, Machines and Drives (PEMD 2018), Liverpool, UK, 17–19 April 2018; pp. 3918–3922.
22. Wu, H.; Ni, H.; Heydt, G.T. The Impact of Time Delay on Robust Control Design in Power Systems. In Proceedings of the IEEE Power Engineering Society Winter Meeting, New York, NY, USA, 27–31 January 2002.
23. Ranjan, S.; Das, D.C.; Behera, S.; Sinha, N. Parabolic trough solar–thermal–wind–diesel isolated hybrid power system: Active power/ frequency control analysis. *IET Renew. Power Gener.* **2018**, *12*, 1893–1903. [[CrossRef](#)]
24. Kennedy, J.; Eberhart, R. *Particle Swarm Optimization*; Purdue School of Engineering and Technology: Indianapolis, IN, USA, 1995; pp. 1–7.
25. Mirjalili, S.; Gandomi, A.H.; Mirjalili, S.Z.; Saremi, S.; Faris, H.; Mirjalili, S.M. Salp Swarm Algorithm: A bio-inspired optimizer for engineering design problems. *Adv. Eng. Softw.* **2017**, *114*, 163–191. [[CrossRef](#)]
26. Arora, S.; Singh, S. Butterfly optimization algorithm: A novel approach for global optimization. *Soft Comput.* **2019**, *23*, 715–734. [[CrossRef](#)]
27. Tungadio, D.H.; Bansal, R.C.; Siti, M.W. Optimal control of active power of two micro-grids interconnected with two AC tie-lines. *Electr. Power Compon. Syst.* **2017**, *45*, 2188–2199. [[CrossRef](#)]

28. Lal, D.K.; Barisal, A.K.; Tripathy, M. Load Frequency Control of Multi Area Interconnected Microgrid Power System using Grasshopper Optimization Algorithm Optimized Fuzzy PID Controller. In Proceedings of the 2018 Recent Advances on Engineering, Technology and Computational Sciences (RAETCS), Allahabad, India, 6–8 February 2018; pp. 1–6.
29. Ei-Fergany, A.A.; Ei-Hameed, A.M. Efficient frequency controllers for autonomous two-area hybrid microgrid system using social-spider optimizer. *IET Gener. Transm. Distrib.* **2017**, *11*, 637–648. [[CrossRef](#)]
30. Bhuyan, M.; Barik, A.K.; Das, D.C. GOA optimised frequency control of solar-thermal/sea-wave/biodiesel generator based interconnected hybrid microgrids with DC link. *Int. J. Sustain. Energy* **2020**, *39*, 615–633. [[CrossRef](#)]
31. Wang, X.; Zhao, Q.; He, B.; Wang, Y.; Yang, J.; Pan, X. Load frequency control in multiple microgrids based on model predictive control with communication delay. *J. Eng.* **2017**, *2017*, 1851–1856. [[CrossRef](#)]
32. Global Review of Solar Tower Technology. August 2014. Available online: <http://www.seriuis.org/pdfs/global-review-solar-tower-technology.pdf> (accessed on 26 August 2020).
33. Cerecedo, L.O.L.; Pitalua-Diaz, N.; Transito, I.S.; Contreras, L.E.V.; Bulnes, C.A. Optical performance modeling of a solar tower heliostat field and Estimation of receiver temperature. In Proceedings of the 2013 IEEE International Autumn Meeting on PE and computing, Mexico City, Mexico, 13–15 November 2013; pp. 1–6.
34. Latif, A.; Das, D.C.; Barik, A.K.; Ranjan, S. Maiden co-ordinated load frequency control strategy for ST-AWEC-GEC-BDDG based independent three-area interconnected microgrid system with combined effect of diverse energy storage and DC link using BOA optimized PFOID controller. *IET Renew. Power Gener.* **2019**, *10*, 2634–2646. [[CrossRef](#)]
35. Tehrani, K. A smart cyber physical multi-source energy system for an electric vehicle prototype. *J. Syst. Archit.* **2020**, *111*, 101804. [[CrossRef](#)]
36. Bendjedja, M.; Tehrani, K.A.; Azzouz, Y. Design of RST and fractional order PID controllers for an induction motor drive for electric vehicle application. In Proceedings of the 7th IET International Conference on Power Electronics, Machines and Drives (PEMD 2014), Manchester, UK, 8–10 April 2014; pp. 1–8.
37. Khezri, R.; Oshnoei, A.; Hagh, M.T.; Muyeen, S.M. Coordination of Heat Pumps, Electric Vehicles and AGC for Efficient LFC in a Smart Hybrid Power System via SCA-Based Optimized FOPID Controllers. *Energies* **2018**, *11*, 420. [[CrossRef](#)]
38. Singh, V.P.; Samuel, P.; Kishor, N. Effect of Communication Delay on Load Frequency Control Application in Autonomous Hybrid Power System. In Proceedings of the 2015 IEEE Innovative Smart Grid Technologies, Bangkok, Thailand, 3–6 November 2015; pp. 1–6.
39. Latif, A.; Hussain, S.M.S.; Das, D.C.; Ustun, T.S. Optimum Synthesis of a BOA Optimized Novel Dual-Stage PI – (1 + ID) Controller for Frequency Response of a Microgrid. *Energies* **2020**, *13*, 3446. [[CrossRef](#)]

